Performance Enhancement of a Solar Photovoltaic System with Differential Evolution-Optimized Quasi Sliding Mode Control

Habiba Rizki[1*], *El-Mahjoub* Boufounas[2], *Aumeur* El Amrani[1], *Mohamed* El Amraoui[3], and *Lahcen* Bejjit[1]

[1]MIN Research Group, LASMAR Laboratory, Higher School of Technology Meknes, Moulay Ismail University of Meknes, Morocco
[2]REIPT Laboratory, Faculty of Sciences and Technology, B.P. 509, Boutalamine, Errachidia, Moulay Ismail University of Meknes, Morocco
[3]LASMAR Laboratory, Faculty of Sciences Meknes, Moulay Ismail University of Meknes, Morocco

Abstract. This paper presents a novel approach to enhancing the performance of a solar photovoltaic (PV) system by integrating a Differential Evolution (DE) optimization algorithm into the design of a Quasi Sliding Mode Controller (QSMC). The proposed method aims to address the challenges associated with Conventional Sliding Mode Control (CSMC), such as chattering and suboptimal tracking accuracy, which can significantly impact the stability and efficiency of PV systems. Simulation results show that the DE-optimized QSMC reduces tracking error to 0.05 V, while conventional SMC results in a tracking error of 0.15 V. Chattering amplitude is also significantly reduced, from 0.12 A to 0.03 A and the response time is improved from 0.8 seconds to 0.5 seconds. By leveraging the robustness of QSMC and the flexibility of DE, the DE-QSMC is fine-tuned to minimize tracking errors, reduce chattering, and maintain optimal performance under varying environmental conditions. The stability of the proposed technique is rigorously analyzed using the Lyapunov function theorem, ensuring robust system behavior. The effectiveness of the DE-optimized QSMC is validated through simulations conducted on the Matlab platform, demonstrating superior performance compared to conventional control techniques.

1 Introduction

Photovoltaic solar energy has become a key element in the global energy transition due to its ability to convert solar radiation directly into clean and sustainable electricity. However, the efficiency of photovoltaic systems is often compromised by variations in environmental conditions, such as solar irradiance and temperature, which directly influence the output voltage of the solar modules [1]. To maximize energy efficiency, it is crucial to stabilize and

* Corresponding author: h.rizki@edu.umi.ac.ma

regulate this output voltage, ensuring that the PV system consistently operates at its Maximum Power Point (MPP) [2].

In addition, the DC-DC boost converter plays a critical role in this regulation by adjusting the output voltage of the PV modules to align with the MPP [2]. This component is essential for managing the inherent nonlinearities of the PV system, which are further complicated by environmental fluctuations. These nonlinearities make MPP tracking a complex task, thus complicating the optimization of energy production. Therefore, the integration of Maximum Power Point Tracking (MPPT) technology is fundamental [3]. This technology dynamically adjusts the voltage to maintain optimal energy production, even under changing conditions.

MPPT is an essential technique for maximizing the energy efficiency of PV systems, ensuring that the PV modules always operate at their optimal efficiency, regardless of variations in irradiance and temperature. Traditionally, methods such as Perturb and Observe (P&O) and the Incremental Conductance (INC) algorithm have been widely used for MPPT [4-5]. Although these traditional methods are simple and easy to implement, they present significant limitations, particularly in terms of slow response, sensitivity to rapid environmental fluctuations, and difficulty in maintaining precise MPPT tracking under dynamic conditions [6].

In response to these challenges, Sliding Mode Control (SMC) has emerged as a robust alternative, capable of maintaining stable performance even in the presence of disturbances and uncertainties [7]. However, traditional SMC has some limitations, the most notable is the phenomenon of chattering, which can induce undesirable oscillations and compromise system stability [8-9]. To address these issues, several advanced SMC techniques have been developed. Integral Sliding Mode Control (ISMC) effectively mitigates the reaching phase problem, enhancing transient response and reducing chattering, especially when combined with a low-pass filter [10-11]. Despite these improvements, residual chattering can still occur due to the inherent switching nature of SMC. Other methods like Terminal Sliding Mode Control (TSMC) and Nonsingular Terminal Sliding Mode Control (NT-SMC) have been proposed to improve convergence time and reduce steady-state errors [12-13]. While these techniques offer certain advantages, they also require careful tuning and may not fully eliminate chattering. Additionally, intelligent control strategies such as fuzzy logic and neural networks have been applied to enhance robustness and maximize PV power output [14-15-16]. However, these methods introduce significant computational complexity and higher implementation costs, making them less practical in some scenarios.

Given these limitations, a need persists for a control strategy that balances robustness, simplicity, and efficiency. Quasi Sliding Mode Control (QSMC) has been introduced as a promising solution, addressing the drawbacks of traditional SMC by reducing chattering and improving system response [17]. Nevertheless, to achieve optimal performance, it is essential to carefully optimize the parameters of the QSMC controller [18]. This optimization process is crucial for fine-tuning the controller's response, minimizing tracking errors, and ensuring robust operation under varying conditions. Several approaches were considered for this purpose, including Genetic Algorithms (GA) [19-20], Particle Swarm Optimization (PSO) [21], and Harris Hawks Optimization (HHO) [22]. While these methods have proven effective in various applications, Differential Evolution (DE) stands out as a particularly powerful and efficient algorithm [23]. Known for its ability to search complex, multi-dimensional spaces, DE offers a robust solution for precisely adjusting QSMC parameters, thereby enhancing the overall performance and stability of the PV system.

In this context, the study presented in this paper introduces an innovative approach by integrating DE optimization into the design of a QSMC controller for the PV system. This method not only minimizes tracking errors and reduces chattering but also significantly enhances system stability and efficiency under varying environmental conditions. What makes this approach particularly innovative is its ability to combine the robustness of QSMC

with the flexibility and effectiveness of DE optimization, providing an advanced and practical solution for controlling PV systems.

This innovative combination of DE optimization and QSMC transcends the limitations of traditional and advanced control techniques, offering a versatile and highly adaptive solution. Unlike conventional methods, which struggle with rapid environmental changes or require complex tuning, DE-QSMC seamlessly adjusts to dynamic conditions, ensuring superior stability and performance. Its ability to fine-tune parameters in real time, without sacrificing simplicity or efficiency, positions it as a cutting-edge tool in the realm of photovoltaic system control.

The remainder of this article is structured as follows: Section 2 presents the mathematical model of the studied PV system, including the PV module, the boost converter, and the overall dynamic model. Section 3 focuses on the design of the QSMC controller, with an emphasis on integrating the DE algorithm for parameter optimization. Section 4 details the simulation results obtained under various environmental conditions, comparing the performance of the DE-QSMC with conventional techniques. Finally, the last section concludes with this study's contributions and suggests future research directions.

2 Mathematical modeling of the PV system

Mathematical modeling is a theoretical approach which remains key to understanding and improving photovoltaic systems. Figure 1 shows the investigated PV system configuration that introduces the PV module and boost converter models, focusing on a standalone PV system with a resistive load [18].

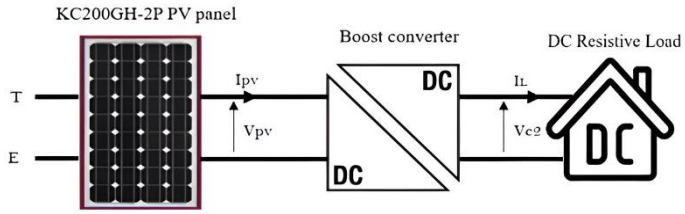

Fig. 1. PV system configuration.

PV cells can be illustrated using either the single-diode or two-diode model, both offering similar efficiency. This work uses the single-diode model for its simplicity and accuracy, as shown in Figure 2 [8].

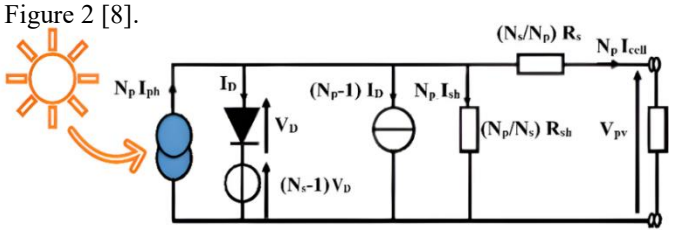

Fig. 2. Single-diode model of the photovoltaic cell.

2.1 PV module modeling

The PV module's electrical behaviour is characterized by the current-voltage relationship, which is essential for understanding the module's performance under varying conditions. The output current I_{pv} can be expressed as follows [18]:

$$I_{pv} = N_p I_{ph} - N_p I_0 \left(\exp\left(\frac{qV_{pv}}{N_s AkT} \right) - 1 \right) \tag{1}$$

where:

- I_{pv} and V_{pv} represent the output current and voltage of the PV module.
- I_{ph} the photocurrent generated by the PV cell, dependent on the incident solar radiation and temperature.
- I_0 and I_{0r} denote the reverse saturation current at the cell temperature T and reference temperature T_r, respectively.
- N_p and N_s represent the module's number of parallels and series cells.
- A is a factor that characterizes the ideality of the p-n junction.
- The Boltzmann constant k is given as 1.3805×10^{-23}J/K.

The reverse saturation current I_0 varies with temperature according to the following expression:

$$I_0 = I_{0r} \left(\frac{T}{T_r} \right)^3 \exp\left(\frac{qE_g}{kT} \left(\frac{1}{T_r} - \frac{1}{T} \right) \right) \tag{2}$$

Here, I_{0r} is calculated as:

$$I_{0r} = \frac{I_{scr}}{\exp\left(\frac{qV_{oc}}{N_s AkT} \right) - 1} \tag{3}$$

where I_{sc} and V_{oc} denote the PV cell's short-circuit current and open-circuit voltage under reference conditions.

The generated photocurrent I_{ph} is influenced by the solar irradiance E and temperature T as follows [18]:

$$I_{ph} = \left(I_{scr} + K_i \left(T - T_r \right) \right) \frac{E}{1000} \tag{4}$$

where K_i is the short-circuit current temperature coefficient.

The power output of the PV module P_{pv}, is the product of the voltage and current, calculated as:

$$P_{pv} = V_{pv} I_{pv} = N_p I_{ph} V_{pv} - N_p I_0 V_{pv} \left(\exp\left(\frac{qV_{pv}}{N_s AkT} \right) - 1 \right) \tag{5}$$

Figure 3 illustrates the PV module's voltage-current and voltage-power characteristics at different levels of solar irradiance and temperature. These curves demonstrate how environmental conditions affect the module's performance. Operating the PV module at its optimal voltage is essential to ensure maximum power output and system efficiency.

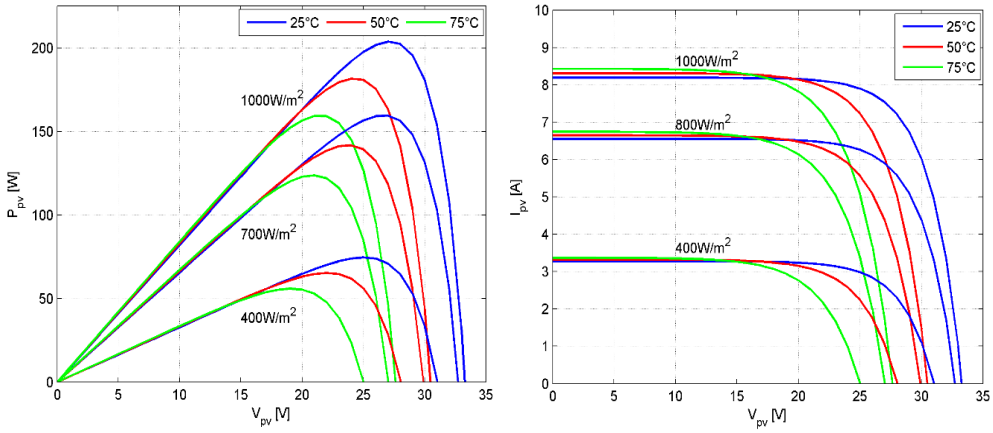

Fig. 3. (a) Power-Voltage and **(b)** Current-Voltage characteristics of the PV module at various temperatures and irradiance levels.

2.2 Boost converter modeling

In a PV system, the boost converter is crucial for regulating the output voltage of solar panels, ensuring optimal energy production and system efficiency. By stabilizing the voltage, particularly during fluctuations in solar irradiance and temperature, the boost converter enables the system to consistently operate near its MPP. The dynamic behaviour of the boost converter, which directly influences the PV module's output voltage V_{pv}, is governed by the following equations [12]:

$$\begin{cases} V_{pv} = \dfrac{1}{C_1}\left(I_{pv} - I_L\right) \\ \dot{I}_L = \dfrac{1}{L}V_{pv} - \dfrac{R_c\left(1-d\right)}{L\left(1+\dfrac{R_c}{R}\right)}I_L + \dfrac{1-d}{L}\left(\dfrac{R_c}{R_c+R}-1\right)V_{C2} - \dfrac{V_D\left(1-d\right)}{L} \\ \dot{V}_{C2} = \dfrac{\left(1-d\right)}{C_2\left(1+\dfrac{R_c}{R}\right)}I_L - \dfrac{1}{C_2\left(R+R_c\right)}V_{C2} \end{cases} \tag{6}$$

Considering that V_{pv} is the voltage generated by the PV module, V_{C2} corresponds to the output voltage of the converter, I_L denotes the inductor current, V_D represents the diode's threshold voltage, d is the duty cycle, R stands for the load resistance, and R_c represents the internal resistance of the capacitor C_2 (Figure 4).

2.3 Dynamic modeling of the PV system

This sub-section introduces the dynamic model of the PV system in state space, which is crucial for developing an effective control strategy. The state variables are defined as [12]:

$$\begin{cases} x_1(t) = V_{pv}(t) \\ x_2(t) = I_L(t) \\ x_3(t) = V_{C2}(t) \\ u(t) = d(t) \end{cases} \tag{7}$$

with the control input *u(t)* representing the duty cycle of the boost converter.
By combining Eqs. (6) and (7), the system's dynamic model is expressed as follows:

$$\begin{cases} \dot{x}_1(t) = \dfrac{1}{C_1}\left(-x_2(t) + I_{pv}\right) \\ \dot{x}_2(t) = f_1(x) + g_1(x)u(t) \\ \dot{x}_3(t) = f_2(x) + g_2(x)u(t) \end{cases} \tag{8}$$

where:

$$\begin{cases} x = [x_1, x_2, x_3]^T \\ f_1(x) = \dfrac{x_1}{L} - \dfrac{R_c}{L\left(1 + \dfrac{R_c}{R}\right)}x_2 + \dfrac{1}{L}\left(\dfrac{R_c}{R + R_c} - 1\right)x_3 - \dfrac{V_D}{L} \\ g_1(x) = -\dfrac{R_c}{L\left(1 + \dfrac{R_c}{R}\right)}x_2 - \dfrac{1}{L}\left(\dfrac{R_c}{R + R_c} - 1\right)x_3 + \dfrac{V_D}{L} \\ f_2(x) = \dfrac{1}{C_2\left(1 + \dfrac{R_c}{R}\right)}x_2 - \dfrac{1}{C_2(R + R_c)}x_3 \\ g_2(x) = -\dfrac{1}{C_2\left(1 + \dfrac{R_c}{R}\right)}x_2 \end{cases} \tag{9}$$

Eq. (8) provides a comprehensive representation of the PV system's dynamic behavior, which is essential for designing the control input signal to ensure that the output voltage V_{pv} consistently tracks the Maximum Power Voltage (MPV). This study focuses on developing a control law that allows the boost converter to maintain this optimal voltage, ensuring efficient and stable operation under varying environmental conditions.

3 Quasi Sliding Mode Controller design

This section presents the design of a Quasi Sliding Mode Controller (QSMC) that aims to enhance response time, reduce chattering, and accurately track the reference voltage V_{ref} with minimal tracking error, ensuring the MPV in the photovoltaic control system. The following schematic illustrates the system setup, showcasing how the control law is generated to maintain stability during disruptions and ensure operation near the MPP.

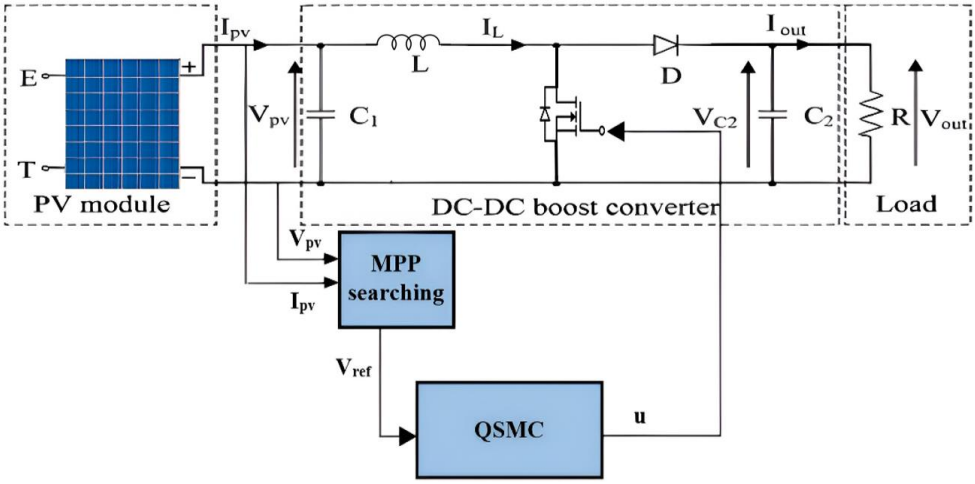

Fig. 4. Schematic diagram of the PV system with QSMC.

3.1 Maximum Power Point Tracking (MPPT)

To achieve MPPT in a photovoltaic (PV) system, it is essential to accurately track the reference voltage V_{ref}, which represents the MPV. The expression for V_{ref} is derived based on the operating conditions of the PV system and is crucial for ensuring that the system operates at its optimal point.

Starting from Eq. (5), the derivative of power with respect to current must be equal to zero, as shown in the following equation:

$$\frac{dP_{pv}(t)}{dI_{pv}(t)} = I_{pv}(t).\frac{dV_{pv}(t)}{dI_{pv}(t)} + V_{pv}(t) = 0 \tag{10}$$

The PV module output voltage V_{pv} can be derived using the PV current I_{pv} expression in Eq. (1) as follows:

$$V_{pv} = \frac{N_s AkT}{q} Log\left(\frac{I_{ph} - I_{pv} + I_0}{I_0}\right) \tag{11}$$

thus:

$$\frac{dV_{pv}}{dI_{pv}} = -\frac{N_s AkT}{q}\frac{1}{I_0 - I_{pv} + I_{ph}} \tag{12}$$

By substituting Eq. (11) and (12) into the Eq. (10), we arrive at the following relationship:

$$Log\left(\frac{I_{ph} - I_{pv} + I_0}{I_0}\right) = \frac{1}{I_{ph} - I_{pv} + I_0} \tag{13}$$

Eq. (13) reveals a linear relationship between the reference current I_{ref} and the photocurrent I_{ph} as follows [18]:

$$I_{ref} = 0.909 I_{ph} \tag{14}$$

Finally, the reference maximum power voltage V_{ref} is obtained by substituting the expression for I_{ref} into Eq. (11) :

$$V_{ref} = \frac{N_s AkT}{q} Log\left(\frac{I_0 - I_{ref} + I_{ph}}{I_0}\right) \tag{15}$$

This final expression for V_{ref} allows the PV system to operate at the MPP, ensuring that the system achieves optimal energy output.

3.2 Quasi Sliding Mode Control (QSMC)

In a PV system, establishing the appropriate control law requires a precise definition of the tracking error, which can be represented as follows:

$$e(t) = V_{ref}(t) - V_{pv}(t) \tag{16}$$

Building on Eq. (16), the sliding surface $\sigma(t)$ is defined as:

$$\sigma(t) = \left(\lambda + \frac{d}{dt}\right)^{r-1} e(t) \tag{17}$$

here, λ is a positive constant, and r represents the relative degree of the system.
For a system with a relative degree $r = 2$, the sliding surface equation simplifies to:

$$\sigma(t) = \dot{e}(t) + \lambda e(t) \tag{18}$$

Using the specified criteria in Eq. (19) guarantees that the system's behavior moves toward the sliding surface and remains strong even under changes in temperature and irradiance conditions.

$$\sigma(t)\dot{\sigma}(t) < -\eta\left|\sigma(t)\right| \tag{19}$$

The derivation of the sliding surface is given by:

$$\dot{\sigma}(t) = \ddot{V}_{ref}(t) + \frac{1}{C_1}\left(f_1(x,t) + g_1(x,t)u(t) - \dot{I}_{pv}(t)\right) + \lambda\dot{e}(t) \tag{20}$$

In CSMC, the use of the discontinuous sign function often leads to high-frequency oscillations that can degrade system performance and mechanical components. To mitigate this issue, the QSMC modifies the control law by introducing an additional term to the derivative of the sliding surface as follows:

$$\dot{\sigma}(t) = -k\,Sat\left(\sigma(t)\right) - \beta\sigma(t) \tag{21}$$

with k and β are positive constants, and $Sat\left(\sigma(t)\right)$ is a saturation function, defined as:

$$Sat\left(\sigma(t)\right) = \begin{cases} \sigma(t)/L & if\ \left|\sigma(t)\right| < L \\ Sign\left(\sigma(t)\right) & otherwise \end{cases} \tag{22}$$

The introduction of the saturation function $Sat\left(\sigma(t)\right)$, along with the added term $-\beta\sigma(t)$, helps to smooth the control action, reduces chattering, and maintains system stability within the boundary layer, ensuring a more refined and robust control response.
The equivalence between Eq. (20) and Eq. (21) allows obtaining the control law for QSMC, which is defined as follows:

$$u(t) = \frac{1}{g_1(x,t)}\left[-f_1(x,t) + \dot{I}_{pv}(t) - C_1\ddot{V}_{ref}(t) - \lambda C_1\dot{e}(t) - kC_1 Sat\left(\sigma(t)\right) - \beta C_1\,\sigma(t)\right] \tag{23}$$

QSMC significantly enhances PV system performance. However, the optimal tuning of gains (k, β, λ) is crucial for perfect control. Proper adjustment is the key to maximizing efficiency and ensuring the system's robustness under varying conditions.

4 Differential Evolution algorithm-based Quasi Sliding Mode Control (DE-QSMC)

In this section, the focus is on employing the Differential Evolution (DE) algorithm to optimize the gains of the QSMC in PV systems. The DE algorithm provides a systematic and efficient method to fine-tune the controller's parameters (k, β, λ), ensuring enhanced performance, stability, and minimal tracking error under varying operating conditions. The DE algorithm operates through the following key steps [23]:

Initialization: A population of potential solutions is randomly generated within predefined bounds. Each individual in the population represents a set of gains (G) for the QSMC, in this study G= {k_i, β_i, λ_i} with (i) denotes the index of the individual in the population.

Mutation: New candidate solutions, known as mutant vectors, are created by combining existing solutions using weighted differences between them. The mutation operation can be expressed as [24]:

$$V_i = G_{r1} + F \cdot (G_{r2} - G_{r3}) \tag{24}$$

where V_i is the mutant vector, G_{r1}, G_{r2}, G_{r3} are randomly selected distinct individuals from the population, and F is the mutation factor that controls the amplification of the differential variation.

Crossover: To introduce variability, the mutant vector V_i is mixed with the current population vector G_i to produce a trial vector U_i. The crossover operation is defined as:

$$U_i = \begin{cases} V_i(j) & \text{if rand}(j) \le C_r \\ G_i(j) & \text{otherwise} \end{cases} \tag{25}$$

Where $\text{rand}(j)$ is a uniformly distributed random number between 0 and 1, and C_r is the crossover rate.

Selection: The trial vector U_i is evaluated using the fitness function, which in this work is the Mean Squared Error (MSE) between the reference voltage V_{ref} and the actual output voltage V_{pv}:

$$\text{MSE} = \frac{1}{n}\sum_{t=1}^{n}(V_{\text{ref}}(t) - V_{\text{pv}}(t))^2 \tag{26}$$

with n is the number of time steps or data points.

If the trial vector U_i achieves a lower MSE, reflecting superior performance, it replaces the corresponding population member G_i in the evolving population. This selective replacement ensures that each generation continually refines the control strategy, driving the system toward optimal performance [25].

$$G_i = \begin{cases} U_i & \text{if MSE}(U_i) < \text{MSE}(G_i) \\ G_i & \text{otherwise} \end{cases} \tag{27}$$

4.1 Proposed intelligent MPPT control strategy

In this sub-section, we proposed an intelligent MPPT control strategy that integrates the Differential Evolution (DE) algorithm with a Quasi Sliding Mode Controller (QSMC).

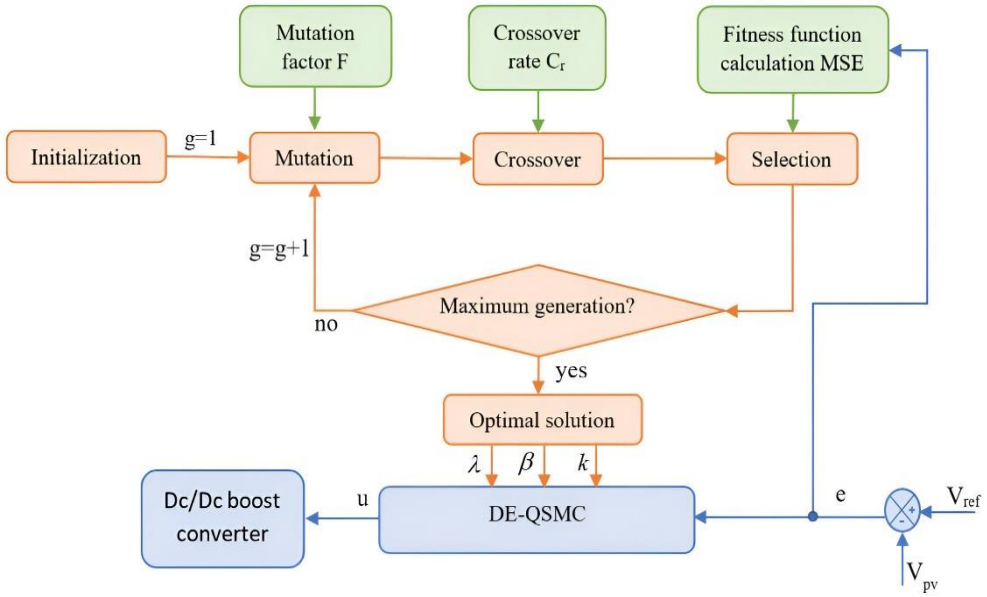

Fig. 6. Flowchart of the DE-QSMC process for optimizing the PV system control parameters.

The flowchart in Figure 6 illustrates the steps involved in applying the DE algorithm to optimize the gains (k, β, λ), thereby enhancing the performance and robustness of the QSMC in achieving efficient MPPT.

Theorem: Given the PV system described by Eq. (8), if the control law is defined as in Eq. (3) and the gains (k, β, λ) are optimized with the DE algorithm, the system states will reach the sliding surface within a specific timeframe, ensuring robust MPPT regardless of varying operating conditions and uncertainties. This approach maximizes the efficiency and reliability of the PV system.

Proof: The stability of the PV system controlled by DE-QSMC is demonstrated by defining the Lyapunov function [18]:

$$V(t) = \frac{1}{2}\sigma^2(t) \tag{28}$$

The derivative of this Lyapunov function is calculated as:

$$\dot{V}(t) = \sigma(t)\dot{\sigma}(t) \tag{29}$$

By substituting $\dot{\sigma}(t)$ with the expression from Eq. (20), the derivative becomes as:

$$\dot{V}(t) = \sigma\left(\ddot{V}_{ref}(t) + \frac{1}{C_1}\left(f_1(x,t) + g_1(x,t)u(t) - \dot{I}_{pv}(t)\right) + \lambda\dot{e}(t)\right) \tag{30}$$

By replacing the control law with its expression defined in the theorem, the Eq. (30) is refined to:

$$\begin{aligned}\dot{V}(t) &= \sigma(t)\left(-k.Sat(\sigma(t)) - \beta\sigma(t)\right)\\ &= -k.\sigma(t).Sat(\sigma(t)) - \beta\sigma^2(t)\\ &< -k.\sigma(t).Sat(\sigma(t))\end{aligned} \tag{31}$$

In the first case when $|\sigma(t)| > L$, $Sat(\sigma(t)) = Sign(\sigma(t))$, the time derivative of the Lyapunov function is given by:

$$\dot{V}(t) < -k|\sigma(t)| < -\eta|\sigma(t)| \text{ , whit } \eta < k \tag{32}$$

this indicates that the Lyapunov function is strictly decreasing, ensuring that the system's state converges to the sliding surface in finite time.

In the second case, when $|\sigma(t)| < L$, $Sat(\sigma(t)) = \frac{\sigma(t)}{L}$, the system's trajectories are confined within a boundary layer around the sliding surface $\sigma(t) = 0$, specifically within a small vicinity around the origin L.

This confirms that the Lyapunov condition is consistently satisfied, driving the tracking error to zero within a finite time and guaranteeing the system's stability and convergence to the sliding surface. Consequently, the control strategy DE-QSMC ensures robust operation, providing accurate and reliable MPPT across different operating conditions.

5 Simulation results and discussions

This section evaluates the effectiveness of the proposed Differential Evolution-based Quasi-Sliding Mode Controller through simulations under various operating conditions. The simulations are conducted on a PV module with parameters outlined in Table 1, with the boost converter parameters detailed in Table 2. These tests compare the performance of DE-QSMC against CSMC and QSMC, under scenarios with sinusoidal irradiation and varying temperatures.

Table 1. Parameters of KC200GH-2P PV module [18].

PV parameter	Value	PV parameter	Value
P_{mppt}	$200W$	V_{oc}	$32.9V$
P_{tol}	$+10/-5\%$	A	1.8
I_{mpp}	$7.61A$	K_i	$4.79mA/°C$
I_{scr}	$8.21A$	N_s	54
V_{mpp}	$26.3V$	N_p	1

Table 2. Parameters of the boost converter [18].

Parameter	Numerical value
L	1.21 mH
C_1 and C_2	1000 μF
R_c	39.6 Ω
R	25 Ω
V_D	20.82 V

5.1 DE optimization process and results

The Differential Evolution (DE) algorithm was employed to optimize the gains of the QSMC for the PV system. The process involved iterative adjustments to minimize the tracking error, reduce chattering, and improve response time, ultimately enhancing overall system stability. The key parameters used in the DE optimization process, such as the mutation factor (F), crossover rate (C_r), number of generations, and population size, are detailed in Table 3.

Table 3. Key Parameters for the DE optimization process.

Parameter	Value
Number of generations	50
Population size	50
Crossover rate	0.9
Mutation factor	0.8

The evolution of the cost function, represented by the Mean Squared Error (MSE), is illustrated in Fig. (7). This figure shows the steady reduction in MSE over successive generations, demonstrating the effectiveness of the DE algorithm in optimizing the control parameters.

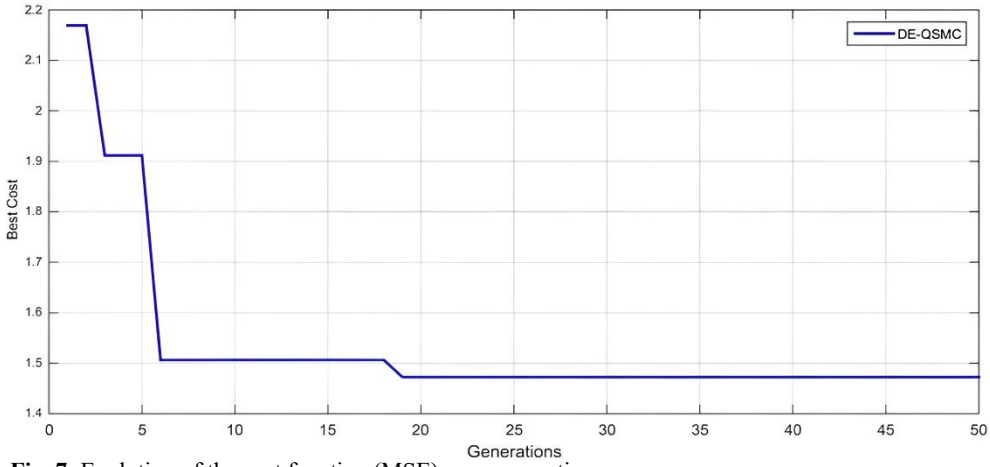

Fig. 7. Evolution of the cost function (MSE) over generations.

Figures 8(a), 8(b), and 8(c) depict the evolution of the gains λ, β, and k, respectively, showing how each gain progresses toward its optimal value during the optimization process.

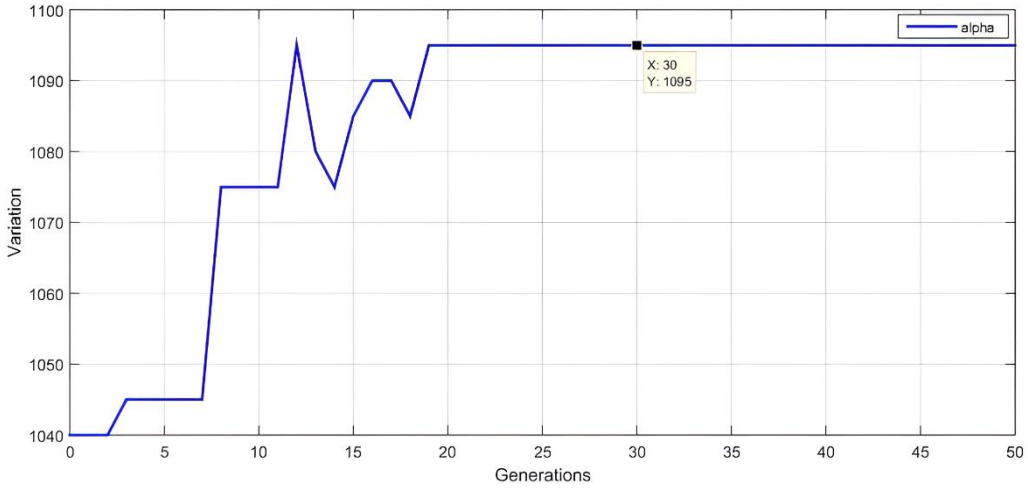

(a)

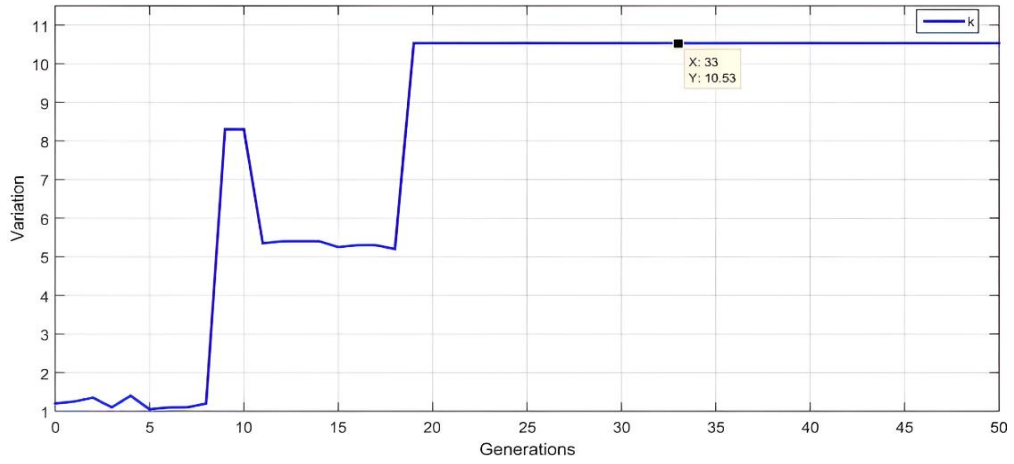

(b)

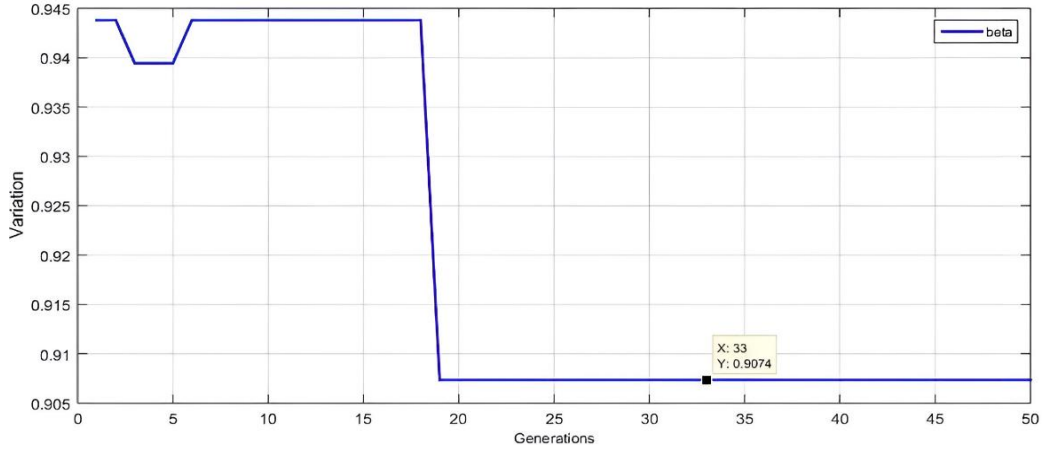

(c)

Fig. 8. (a) Evolution of gain λ, **(b)** gain k, and **(c)** gain β during the optimization process.

Figures 7 and 8 show that the most significant optimization occurred before the 19th generation, where the cost function (MSE) sharply declined, reflecting rapid progress. After this point, the gains and the cost function both stabilized, indicating that the Differential Evolution algorithm successfully optimized the controller. This led to minimized tracking errors and enhanced control stability. The final optimized values of the gains obtained through the DE algorithm are summarized in Table 4.

Table 4. Optimized gain values of DE-QSMC

Parameter	Value
β	0.90
k	10.53
λ	1095

5.2 Simulation under sinusoidal irradiance and variable temperature profile

This sub-section simulates the PV system under a sinusoidal irradiance profile and a stepwise changing temperature profile over the period from 8 AM to 6 PM to compare the effectiveness of three control strategies: CSMC, QSMC, and DE-QSMC.
The irradiance *E(t)* can be expressed by the following sinusoidal equation:

$$E(t) = E_{\max} \cdot \sin\left(\frac{\pi \cdot (t-6)}{12}\right) \tag{33}$$

whit the peak irradiance E_{max} =1000W/m^2, and (t) represents the time in hours.
The temperature *T(t)* changes according to the following step function:

$$T(t) = \begin{cases} 293\ Kelvin = 20^{\circ}\mathrm{C} \\ 308\ Kelvin = 35^{\circ}\mathrm{C} \\ 318\ Kelvin = 45^{\circ}\mathrm{C} \end{cases} \tag{34}$$

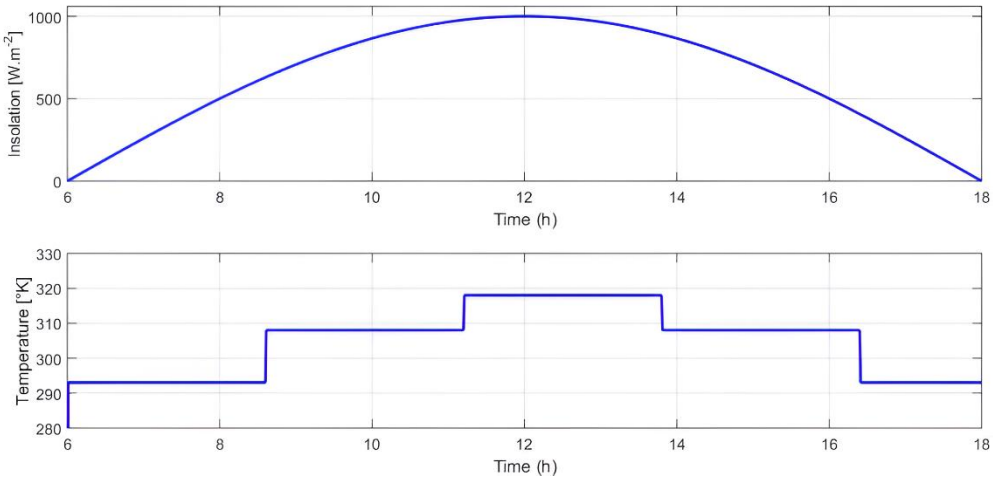

Fig. 9. Profiles of insolation and temperature.

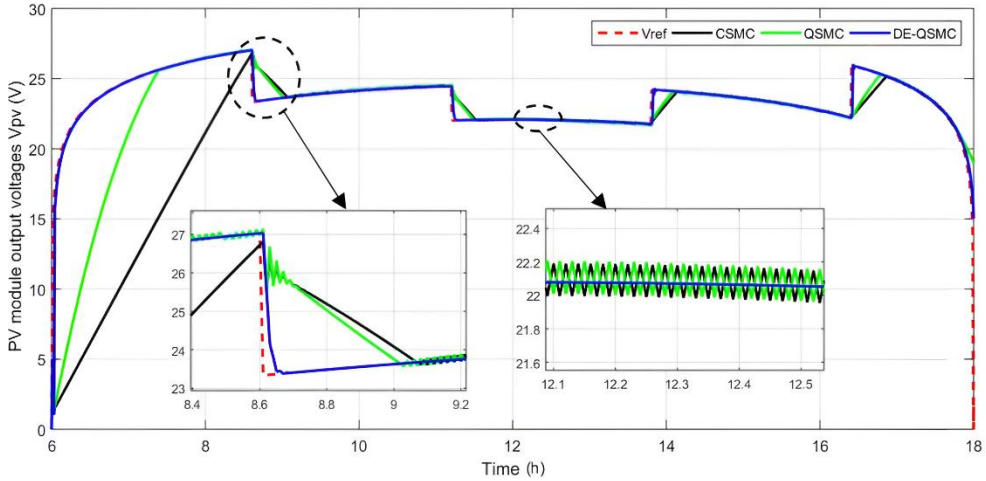

Fig. 10. PV module output voltages under CSMC, QSMC, and DE-QSMC control strategies.

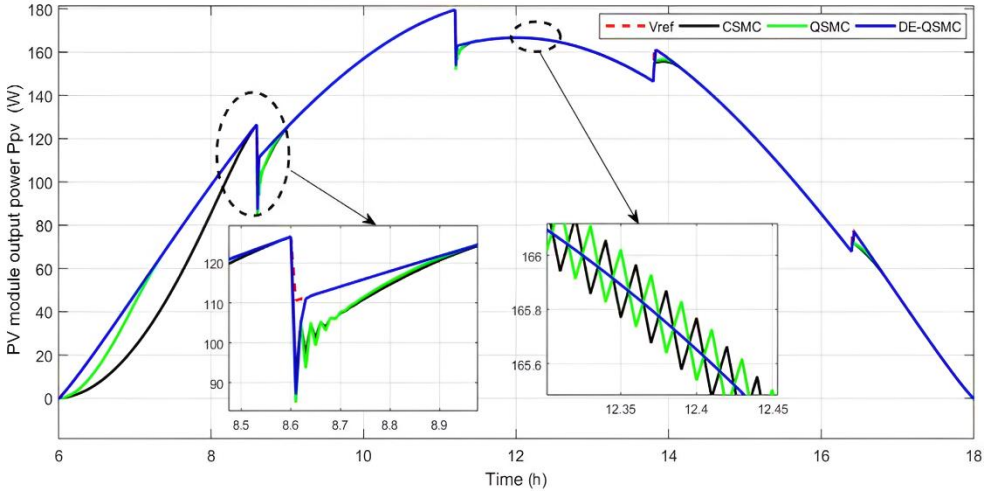

Fig. 11. PV module output power under CSMC, QSMC, and DE-QSMC control strategies.

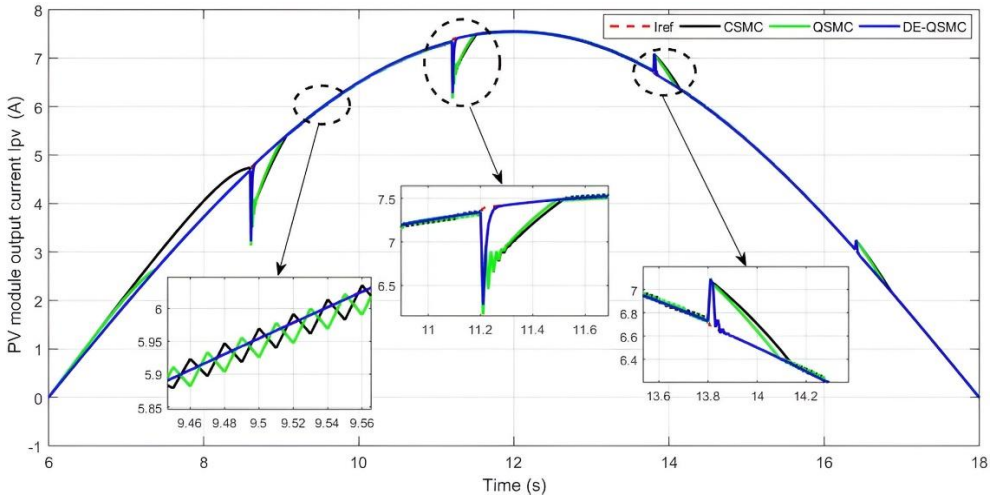

Fig. 12. PV module output current under CSMC, QSMC, and DE-QSMC control strategies.

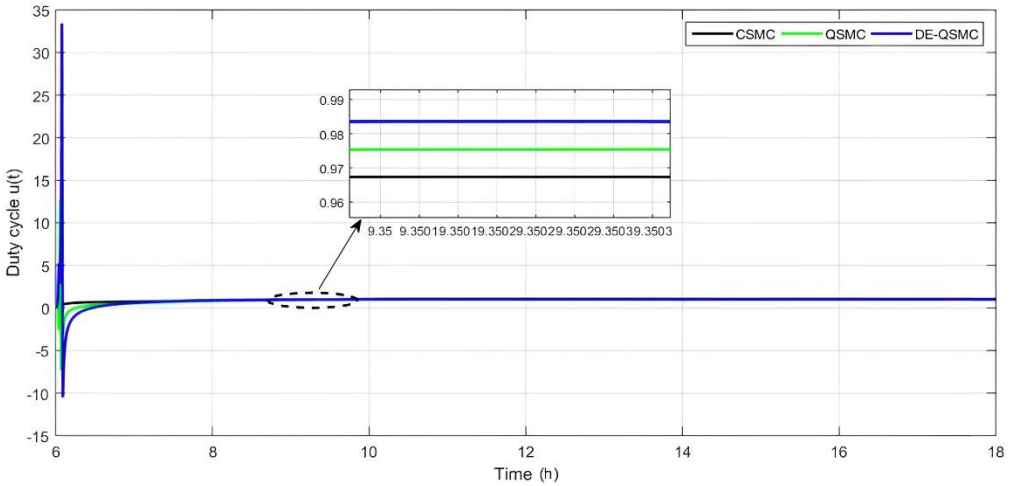

Fig. 13. Duty cycle of the PV system under CSMC, QSMC, and DE-QSMC control strategies.

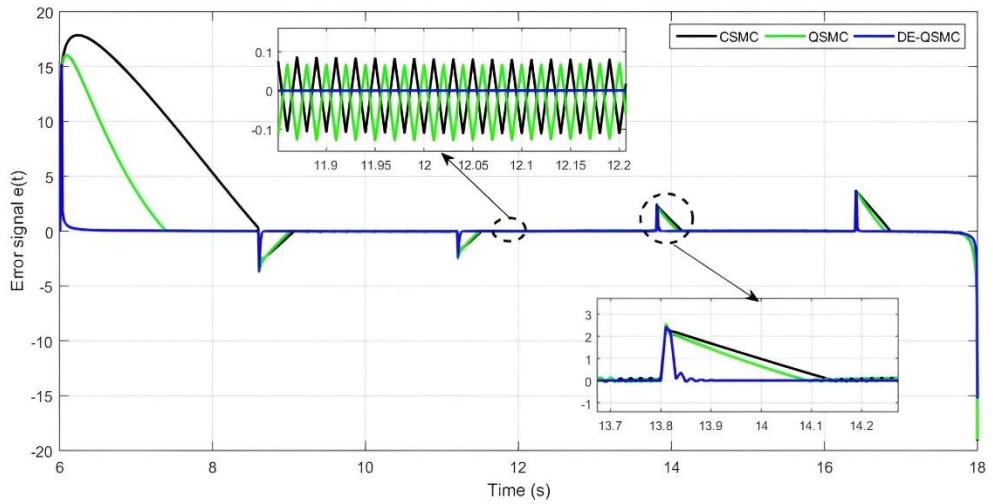

Fig. 10. Tracking error of the PV system under CSMC, QSMC, and DE-QSMC control strategies.

The simulation results associated to the investigated photovoltaic system under varying irradiance and temperature profiles provide a comprehensive view of the system's output voltage V_{pv}, current I_{pv}, and power P_{pv}. The QSMC method demonstrates a marked improvement in response time compared to CSMC, showcasing its ability to adapt more quickly to changes in environmental conditions. However, despite this increase in response time, QSMC still faces significant challenges in maintaining accurate tracking and eliminating the chattering phenomenon, particularly under fluctuating conditions, which impacts the system stability, and damages mechanical components.

In contrast, the DE-QSMC addresses these shortcomings by providing a more refined control approach. By optimizing control parameters using the DE algorithm, DE-QSMC achieves a faster response time and reduced tracking error. More importantly, DE-QSMC eliminates the chattering issue, a common drawback of Conventional Sliding Mode Controllers. The smooth adjustments in the duty cycle under DE-QSMC further contribute to the system's overall precision, ensuring that the control signals are stable and effective. These results confirm DE-QSMC's superior performance in maintaining stable and efficient PV system operation, even under dynamic and challenging environmental conditions.

6 Conclusion

This study has introduced an innovative approach to improving the control of a photovoltaic system by integrating Differential Evolution (DE) optimization with Quasi Sliding Mode Control (QSMC). The proposed DE-optimized QSMC has demonstrated its ability to effectively address the limitations of Conventional Sliding Mode Control (CSMC), particularly by minimizing chattering and enhancing tracking accuracy. Through rigorous analysis using the Lyapunov function theorem, the stability of the proposed method has been confirmed, ensuring robust performance under varying environmental conditions.
In addition, simulation results conducted on the Matlab platform have further validated the superiority of the DE-optimized QSMC, showcasing significant improvements in system stability, response time, and overall efficiency compared to conventional control methods. This approach not only leverages the inherent robustness of SMC but also benefits from the flexibility and effectiveness of DE optimization, making it a practical and advanced solution for PV system control. Lastly, integrating intelligent optimization techniques such as DE into traditional control strategies like QSMC represents a promising direction for future research and development in PV systems. Future work could focus on integrating the DE-QSMC approach with energy storage systems to enhance energy efficiency and reliability. Additionally, developing multi-objective optimization frameworks and incorporating adaptive control strategies, such as machine learning-based predictive models, could offer more responsive and intelligent control under dynamic conditions.

Acknowledgments

The first author would like to thank the National Center for Scientific and Technical Research (CNRST) for the financial support received as part of the "PhD-Associate Scholarship-PASS" program.

References

1. A.O.M. Maka, J.M. Alabid, Solar energy technology and its roles in sustainable development, Clean Energy **6**, 476–483 (2022)
2. M.A.V. Rad, A. Kasaeian and O. Mahian, Evaluation of stand-alone hybrid renewable energy system with excess electricity minimizer predictive dispatch strategy, Energy Conversion and Managemen **299**, 117898 (2024)
3. M.L. Katche, A.B. Makokha, S.O. Zachary, M.S. Adaramola, Comprehensive Review of Maximum Power Point Tracking (MPPT) Techniques Used in Solar PV Systems, Energies **16**, 2206 (2023)
4. N. Zhani, H. Mahmoudi, Comparison of the performance of MPPT control techniques (Fuzzy Logic, Incremental Conductance and Perturb & Observe) under MATLAB/Simulink, IFAC-PapersOnLine **58**, 617-623 (2024)
5. D.A. Asoh, B.D. Noumsi, E.N. Mbinkar, Maximum Power Point Tracking Using the Incremental Conductance Algorithm for PV Systems Operating in Rapidly Changing Environmental Conditions, Smart Grid and Renewable Energy **13**, 89–108 (2022)
6. F.Z. El Hamzaoui *, T. Abderrahime, B.D. Taoufi, Comparison Between Perturb & Observe, Fuzzy Logic MPPT Technique, and The Artificial Neural Network Techniques at Different Temperature Conditions, IFAC-PapersOnLine **58**, 599-604 (2024)
7. Y. Zhang, Y.J. Wang, J.Q. Yu, A Novel MPPT Algorithm for Photovoltaic Systems Based on Improved Sliding Mode Control, Electronics **11**, 2421 (2022)
8. M.R. Mostafa, N.H. Saad, A.A. El-Sattar, Tracking the maximum power point of PV array by sliding mode control method, Ain Shams Engineering Journal **11**, 119-131 (2020)
9. F.F. Ahmad, C. Ghenai, A. K.Hamid, M. Bettayeb, A Novel MPPT Application of sliding mode control for maximum power point tracking of solar photovoltaic systems: A comprehensive review, Annual Reviews in Control **49,** 173-196 (2020)
10. A. Kihal, F. Krim, A. Laib, B. Talbi, H. Afghoul, An improved MPPT scheme employing adaptive integral derivative sliding mode control for photovoltaic systems under fast irradiation changes, ISA Transactions **87**, 297-306 (2019)
11. K. Belamfedel Alaoui, E-M. Boufounas, I. Boumhidi, Integral Sliding Mode Control without Reaching Phase for a variable Speed Wind Turbine, IEEE 2nd International Conference on Electrical and Information Technologies, Rabat Morocco, 78 – 83 (2016)
12. F-E. Lamzouri, E-M. Boufounas, A. Brahmi, A. El Amrani, Optimized TSMC Control Based MPPT for PV System under Variable Atmospheric Conditions Using PSO Algorithm, Procedia Computer Science **170**, 887-892 (2020)
13. M. Maaruf, M. Shafiullah, A.T. Al-Awami, F.S. Al-Ismail, Adaptive Nonsingular Fast Terminal Sliding Mode Control for Maximum Power Point Tracking of a WECS-PMSG, Sustainability **13**, 13427 (2021)
14. K. Ullah, M. Ishaq, F. Tchier, H. Ahmad, Z. Ahmad, Fuzzy-based maximum power point tracking (MPPT) control system for photovoltaic power generation system, Results in Engineering **20**, 101466 (2023)
15. C.G.V. Mier, J.R. Resendiz, J.M.Á. Alvarado, H.R. Resendiz, A.M.H. Navarro, O.R. Abreo, Artificial Neural Networks in MPPT Algorithms for Optimization of Photovoltaic Power Systems: A Review, Micromachines **12**, 1260 (2021)
16. E-M. Boufounas, J. Boumhidi and I. Boumhidi, Optimal H∞ control without reaching phase for a variable speed wind turbine based on fuzzy neural network and APSO algorithm, International Journal of Modelling, Identification and Control **24**, 100-109 (2015)

17. P.K. Mishra, P. Jagtap, Approximation- and Chattering-Free Quasi Sliding-Mode Control for Unknown Systems, IEEE Transactions on Circuits and Systems II: Express Briefs **71**, 3081-3085 (2024)
18. H. Rizki, E.M. Boufounas, A.E. Amrani, M.E. Amraoui, L. Bejjit, Integral Quasi Sliding Mode Control for MPPT of a Standalone Photovoltaic System Without Storage, 2024 4th International Conference on Innovative Research in Applied Science, Engineering and Technology (IRASET), FEZ, Morocco,1-8 (2024)
19. S.R.D. Naoussi, K.T. Saatong, R.J.J. Molu, W.F. Mbasso, M. Bajaj, M. Louzazni, M. Berhanu, S.Kamel, Enhancing MPPT performance for partially shaded photovoltaic arrays through backstepping control with Genetic Algorithm-optimized gains. Sci Rep **14**, 3334 (2024)
20. Y. Berrada, E-M. Boufounas and I. Boumhidi, Optimal neural network sliding mode control without reaching phase using genetic algorithm for a wind turbine, 10th IEEE International Conference on Intelligent Systems: Theories and Applications (SITA'15), ENSIAS, Rabat Morocco,1-6 (2015)
21. I. Bouchrihaa, A. BenGhanem, K. Nour, Optimization of the Sliding Mode Control (SMC) with the Particle Swarm Optimization (PSO) Algorithm for Photovoltaic Systems Based on MPPT, Advances in Science, Technology and Engineering Systems Journal **7**, 100-106 (2022)
22. M.A. Hafeez, A.Naeem, M. Akram, M.Y. Javed, A.B. Asghar, Y.Wang, A Novel Hybrid MPPT Technique Based on Harris Hawk Optimization (HHO) and Perturb and Observer (P&O) under Partial and Complex Partial Shading Conditions. Energies **15**, 5550 (2022)
23. A. P. Firmanza, M. N. Habibi, N. A. Windarko and D. S. Yanaratri, Differential Evolution-based MPPT with Dual Mutation for PV Array under Partial Shading Condition, 2020 10th Electrical Power, Electronics, Communications, Controls and Informatics Seminar (EECCIS), 198-203 (2020)
24. S. Yuan, Y. Ji, Y. Chen, X. Liu, and W. Zhang, An Improved Differential Evolution for Parameter Identification of Photovoltaic Models, Sustainability **15**, 13916 (2023)
25. C. Fu, L. Zhang, A differential evolution optimization-based black widow spider method in PV systems under shading conditions, Applied Soft Computing **148**, 110927 (2023)